AN EXAMINATION OF THE EFFECT OF THE VARIABLE PART OF BLADE CIRCULATION ON THE INDUCED POWER REQUIREMENTS OF A TWO-BLADED ROTOR IN FORWARD FLIGHT BY AN ELECTROMAGNETIC ANALOG

A THESIS

Presented to

the Faculty of the Graduate Division

by

William L. Corley, Sr.

In Partial Fulfillment

of the Requirements for the Degree

Master of Science in Aeronautical Engineering

Georgia Institute of Technology

September, 1961

"In presenting the dissertation as a partial fulfillment of the requirements for an advanced degree from the Georgia Institute of Technology, I agree that the Library of the Institution shall make it available for inspection and circulation in accordance with its regulations governing materials of this type. I agree that permission to copy from, or to publish from, this dissertation may be granted by the professor under whose direction it was written, or, in his absence, by the dean of the Graduate Division when such copying or publication is solely for scholarly purposes and does not involve potential financial gain. It is understood that any copying from, or publication of, this dissertation which involves potential financial gain will not be allowed without written permission.

7A
12R

AN EXAMINATION OF THE EFFECT OF THE VARIABLE PART OF BLADE CIRCULATION ON THE INDUCED POWER REQUIREMENTS OF A TWO-BLADED ROTOR IN FORWARD FLIGHT BY AN ELECTROMAGNETIC ANALOG

Approved:

Date Approved by Chairman: September 5, 1961

ACKNOWLEDGMENTS

I would like to express my sincere appreciation to Dr. Robin B. Gray for his assistance in conducting this study. Also, gratitude is extended to Professor Walter Castles, Jr. for selection of the topic. To Dr. Thomas W. Jackson of the Engineering Experiment Station and Professor Howard L. Durham, I would like to express my appreciation for reviewing and commenting on this thesis. Thanks are extended to Dr. Frank O. Nottingham of the School of Electrical Engineering for designing the current transformers used in the electromagnetic analog.

TABLE OF CONTENTS

LIST OF FIGURES

LIST OF SYMBOLS

A	area of the rotor disc
B	magnetic flux density
b	number of blades of the rotor
C_T	rotor thrust coefficient $\quad C_T = \dfrac{T}{\rho \pi \Omega^2 R^4}$
C_{P_I}	induced power coefficient
M_T	rotor thrust moment
MR	meter reading, decibels
N	subscript for a value at the reference point
n	number of turns of wire on the reference coil
P	subscript for a value at an arbitrary point P
P_I	induced power
R	rotor radius
R_c	radius of reference coil
R_m	wire model rotor radius
r	radial distance from rotor axis
T	rotor thrust
U_T	tangential component of resultant velocity at blade element, $U_T = \Omega r + \mu \Omega R \sin \psi$
V	forward velocity of rotor
V_i	component of induced velocity normal to the rotor plane
w	component of induced velocity normal to the rotor plane
x	non-dimensional radial distance along blade, r/R
α	rotor tip-path angle of attack
Γ	total blade circulation

Γ_o constant part of blade circulation

Γ_1 variable part of blade circulation

γ non-dimensionalized circulation strength, $\gamma = \dfrac{\Gamma}{2C_T \Omega \pi R^2}$

μ rotor tip speed ratio, $\mu = \dfrac{V \cos \alpha}{\Omega R}$

ρ mass density of air

χ wake skew angle, angle between axis of wake and rotor tip-path plane

ψ azimuth angle of blade feathering axis measured from downwind position and in direction of blade rotation

Ω rotor angular velocity

SUMMARY

A wire model of the wake vortices of a rotor blade in forward flight at a blade tip forward speed ratio, μ, of 0.3, and wake skew angle, χ, of 90° was constructed to simulate constant circulation across the rotor blade and lateral harmonic variation in circulation with each 30° azimuth position of the blade.

Electrical current, analogous to the non-dimensionalized values of constant and variable blade circulation, was passed through the wire model and the component of the magnetic field strength normal to the tip-path plane was measured across the rotor diameter for each 30° blade azimuth angle. These measured components of magnetic field strength were converted to induced velocities, non-dimensionalized in terms of the rotor radius and blade circulation. From symmetry and the principle of superposition, the effect of the second blade was obtained to give the total value for a two-bladed rotor. This procedure was repeated using only the vortices shed at the blade root and tip to obtain the effect of only constant circulation across the blade.

The measurements were used in numerically integrating the induced power coefficient equation to obtain a comparison of the effect of assuming lateral harmonic variations in blade circulation, as opposed to assuming only constant circulation, on the induced power requirements of a two-bladed rotor in forward flight at a blade tip forward speed ratio of 0.3.

The results indicate that by assuming only constant circulation, the induced power requirements are underestimated by 16.5 per cent.

CHAPTER I

INTRODUCTION

The wake pattern of a lifting rotor operating in forward flight has been shown to consist of continuous skewed helical vortex filaments caused by the variation in blade vortex strength along the blade radius and closed, pie-shaped vortex filaments caused by the harmonic change of blade bound vortex strength with azimuth angle. An illustration of these filaments, obtained from Reference 1, is given in Fig. 1. Consideration of the pie-shaped vortex filaments, or the variable part of blade circulation, in computing the induced velocity of a rotor has largely been neglected in theory. Also, little consideration has been given to the effect of these pie-shaped vortices on the variations in blade bending stresses across the rotor.

In this study an examination of the effect of the lateral harmonic variations of blade circulation at 30° azimuth angles will be made by using the results obtained from an electromagnetic analog to compare the induced power requirements of a two-bladed rotor in forward flight at a rotor tip forward speed ratio of 0.3 with that computed for a similar rotor assuming only constant blade circulation.

CHAPTER II

APPARATUS AND EXPERIMENTAL PROCEDURE

The equipment used for the experimental portion of this thesis consisted of the following components:

1. The primary coil (wire model of the helical and pie-shaped vortex filaments);
2. The reference coil;
3. The secondary coil (search coil);
4. The amplifier and output meter;
5. The power supply.

Primary Coil.--The primary coil, shown in Fig. 2, was constructed of No. 17 gage, Brown and Sharpe copper wire to represent the helical and pie-shaped vortex filaments. Since the wake skew angle, χ , was assumed to be 90°, the wake extended directly behind the rotor. The rotor radius was ten inches, with the blade extending from the 0.2 radius. Since uniform blade bound vortex strength was assumed along the radius, helical vortex filaments were shed at the blade tip and 0.2 radius. These helical vortex filaments, or constant part of blade bound vortex strength, were represented by a continuous circuit with an arbitrary constant current of 3.0 amperes. The pie-shaped vortex filament strengths, or variable part of the blade bound vortex strength, were calculated over 30° intervals and were represented with a current equivalent to the ratio of the variable and constant blade circulation multiplied by the 3.0 amperes. Since the variable part of the blade

bound vortex strength is a function of $\sin \psi$, the pie-shaped filaments could be represented by three circuits, arranged to give a reduction in field strength from $\psi = 0°$ to $\psi = 180°$ and an addition of field strength from $\psi = 180°$ to $\psi = 360°$. An illustration of these circuits is given in Fig. 6. The correct current was obtained in the circuits by using current transformers that were wound in a ratio of the constant to the variable part of the blade bound vortex strength. In order to simplify the model, the vortices from only one blade were constructed and the results for two blades were obtained by superposing the computed non-dimensionalized values of induced velocity, obtained from measurements taken across the diameter of the rotor.

Reference Coil.--The reference coil consisted of nine closely spaced turns of No. 17 gage wire wrapped on a plexiglas ring. A switching arrangement was used so that the coil could be placed in any of the four circuits. This allowed a check to be made of the current ratios. The meter readings were referenced to the magnetic field strength at the center of the reference coil while in the 3.0 ampere circuit. The reference coil is shown in Fig. 3.

Search Coil.--The search coil consisted of 1000 turns of No. 40, Brown and Sharpe, copper wire wound on a plexiglas core which was mounted on a plexiglas support as shown in Fig. 4. The coil had a diameter of 0.35 inches to the center of the wire bundle which had a cross section approximately 0.09 inches square. A co-axial cable was used to connect the search coil to the amplifier.

Amplifier and Output Meter.--The pickup circuit included a commercial standing wave indicator in addition to the search coil and co-axial cable

described above. This indicator, which had a maximum sensitivity of 0.1 microvolt, consisted of an indicating meter, a high-gain 400 cycle fixed frequency amplifier with a calibrated gain control covering a 60 decibel range, and a narrow 400 cycle band-pass-filter network which had a sharp cutoff at 400 $\pm$ 5 cycles per second. The input impedance of the amplifier was 200,000 ohms, sufficient to eliminate any calibration of the meter scale. The amplifier was placed in a separate room from the model to eliminate any appreciable magnetic coupling from these coils. The standing wave indicator is shown in Fig. 5.

Power Supply.--The power supply was a 400 cycle, 115 volt, aircraft alternator driven by a synchronous motor. A variable resistor was adjusted to allow 3.0 amperes of current to flow in the circuit and enough capacitance was placed in parallel with the circuit to obtain a power factor of unity. The power supply and current transformers were in a different room from the wake model to minimize direct magnetic coupling effects. A wiring diagram of the system is shown in Fig. 7.

Field Survey Procedure.--The search coil was placed directly over the wake model and was aligned so as to pick up only the normal component of the magnetic field strength. With the rotor blade initially in the position of $\psi = 90°$, measurements were made from $r/R = 1.10$ to $r/R = 0.00$. Then by measuring from $r/R = 0.00$ to $r/R = 1.10$ for $\psi = 270°$, the effect of the blade at $\psi = 90°$ on the blade at $\psi = 270°$ could be superposed on the measurements taken when the blade was actually in the $\psi = 270°$ position. The blade position was changed by cutting out 30° of the circuit and re-wiring for each survey.

Twelve surveys were conducted to obtain the non-dimensional nor-

mal component of induced velocity over the entire rotor. Prior to each survey the equipment was allowed a thirty minute warm-up period and the search coil was centered in the plane of the reference coil to obtain an adjusted reference meter reading.

Reduction of Data.--The output meter was calibrated in decibels and it was necessary to convert the meter readings into equivalent values of the non-dimensional normal component of induced velocity. This conversion was accomplished through the following formulas, derived in Reference 2.

$$\frac{B_P}{B_N} = \frac{\text{antilog } 0.1\ (MR)_P}{\text{antilog } 0.1\ (MR)_N}$$

$$\frac{wR}{\Gamma} = \frac{n}{2}\left(\frac{R_m}{R_c}\right)\frac{B_P}{B_N}$$

where B_P magnetic flux density at point under consideration

B_N magnetic flux density at center of reference coil

MR meter reading, decibels

w component of induced velocity normal to the rotor disc

R rotor radius

n number of turns on reference coil

R_m wire model rotor radius

R_c radius of reference coil

The direction of the induced velocity was determined from the vortex geometry and a study of the trends in the experimental data.

CHAPTER III

RESULTS

Figures 8(a) through 8(f) show the non-dimensionalized values of the normal component of induced velocity across the rotor diameter of a two-bladed rotor in forward flight at a rotor tip ratio of 0.3. These values were obtained assuming lateral harmonic variations in blade circulation with each 30 degree azimuth angle and also by assuming constant blade circulation. A comparison of the effect of assuming harmonic variations in blade circulation on the induced power requirements of a two-bladed rotor was obtained by numerically integrating the induced power coefficient equation

$$C_{P_i} = \frac{b\Gamma}{4\pi^2 R^3} \int_0^{2\pi} \int_{.2}^{1} V_i \, F(x, \psi) \, dx \, d\psi$$

$$F(x, \psi) = (2 - 3\mu \sin \psi)(x + \mu \sin \psi)$$

utilizing the data from Fig. 8(a) through 8(f). The induced power coefficient equation was obtained from Appendix C of Reference 1.

The results of this numerical integration indicate that if only constant circulation is assumed, the induced power required by a two-bladed rotor in forward flight at a blade tip forward speed ratio of 0.3 will be underestimated by 16.5 per cent.

CHAPTER IV

CONCLUSIONS

The accuracy of the experimental measurements of this study is not known. The greatest source of error is probably in assuming a wake skew angle of 90 degrees. The electromagnetic analog method has certain inherent inaccuracies as noted in Reference 2:

1. Small variations in primary coil current and frequency;
2. Search coil positioning errors and associated meter reading errors;
3. Inaccuracies in the meter and amplifier calibration;
4. Small distortion in the portion of the model magnetic field of interest arising from the laboratory structure;
5. Errors in plotting and drawing the graphs.

There is no known mathematical solution of this study to use for comparative purposes, but it is stated in Reference 1 that an approximate computation of the induced power required for rotors having one, two, three, and four blades and operating at $\mu = 0.2$ and $\mu = 0.4$, respectively, indicates that previous methods underestimate the induced power by an amount which increases with μ and decreases with the number of blades. For the case mentioned above, the per cent underestimation in induced power required is about 39%, 17%, 6%, and 6% for $\mu = 0.2$ and 71%, 18% and 15% for $\mu = 0.4$. The results of this study support the approximate computations of Reference 1.

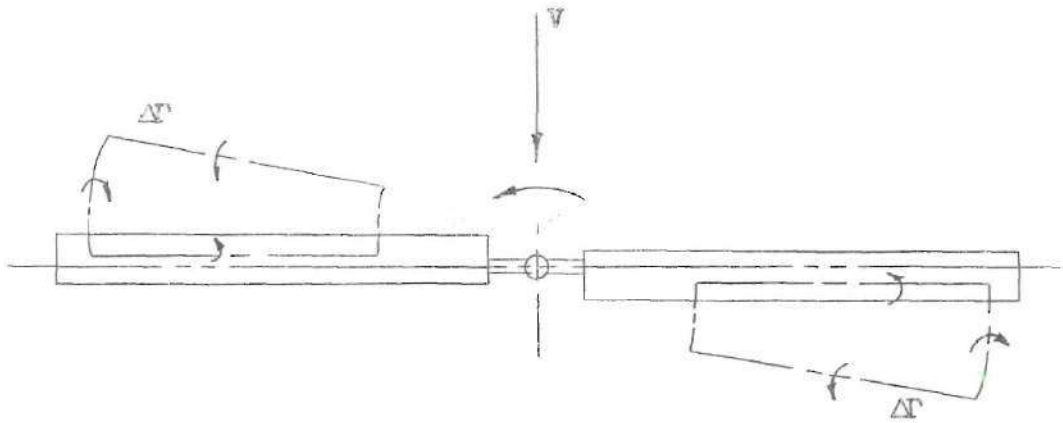

Pie-Shaped Vortices

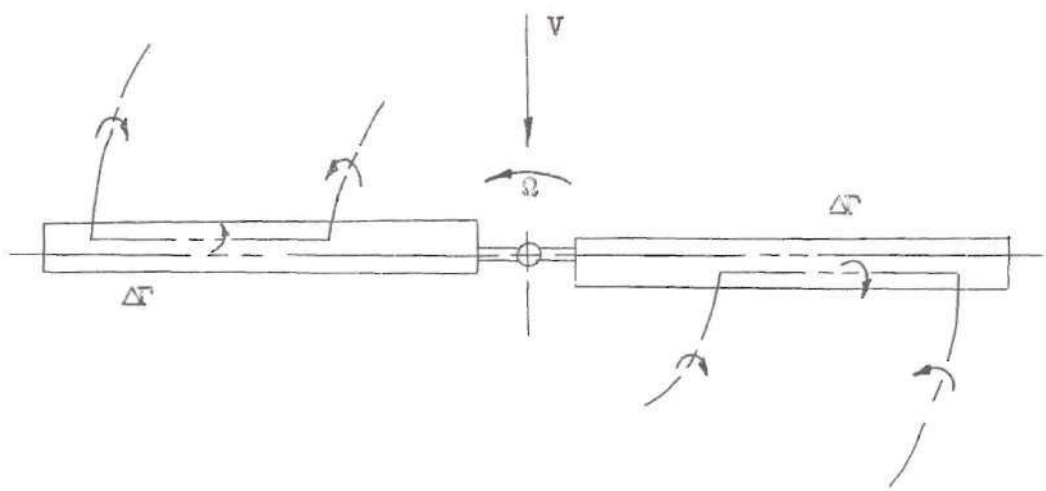

Helical Vortices

Fig. 1 Helical and Pie-Shaped Vortices

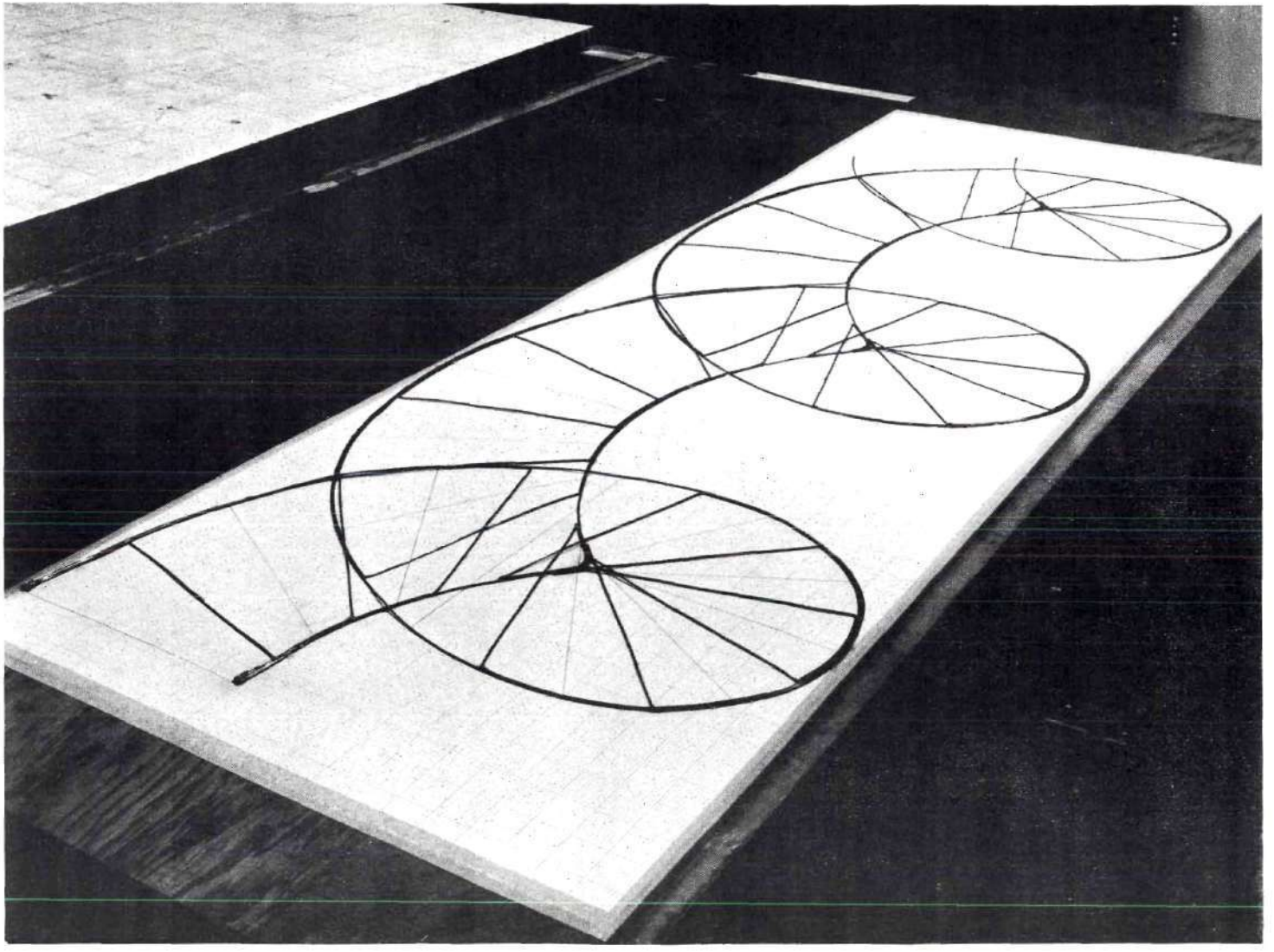

Figure 2. Primary Coil (Wake Model).

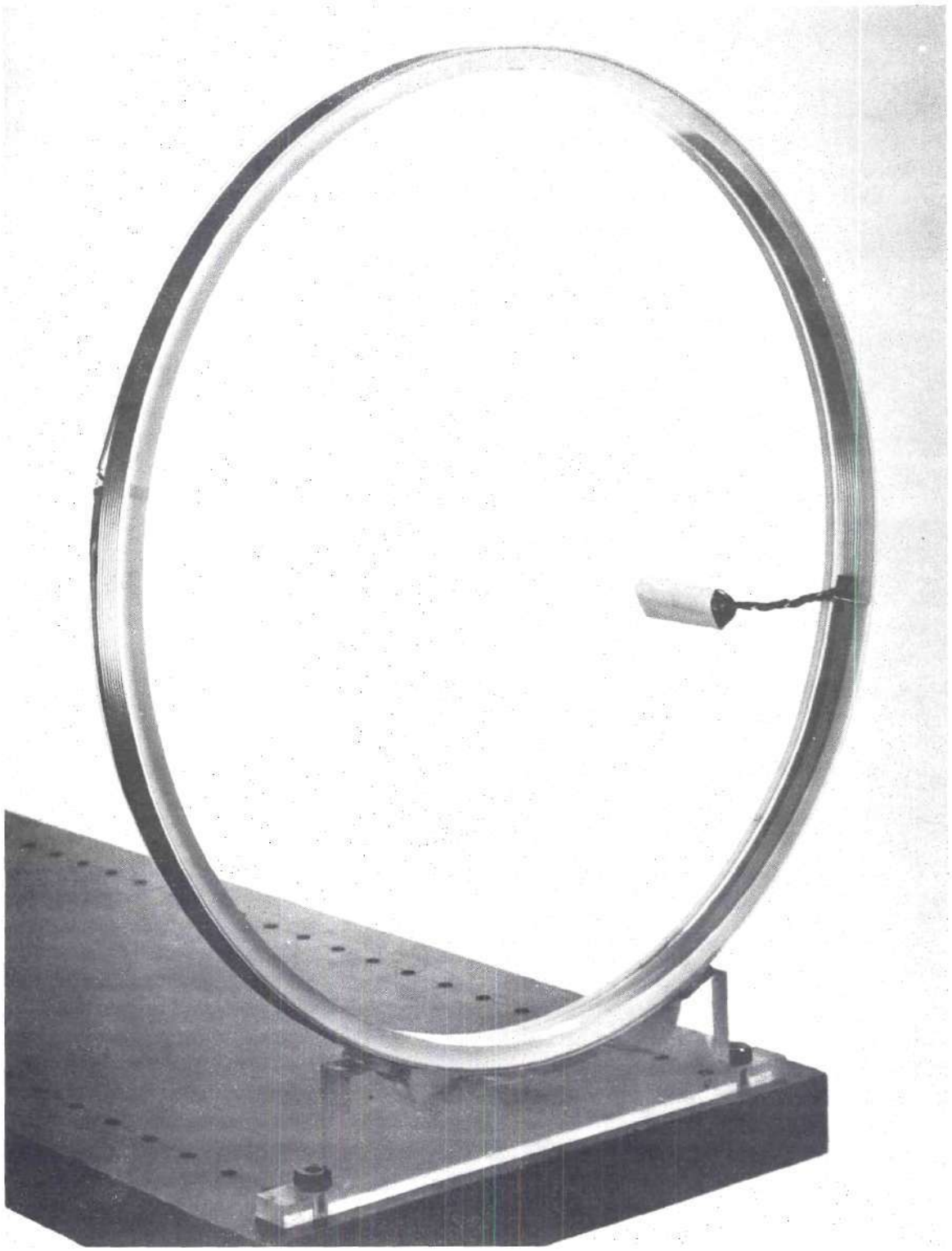

Figure 3. Reference Coil.

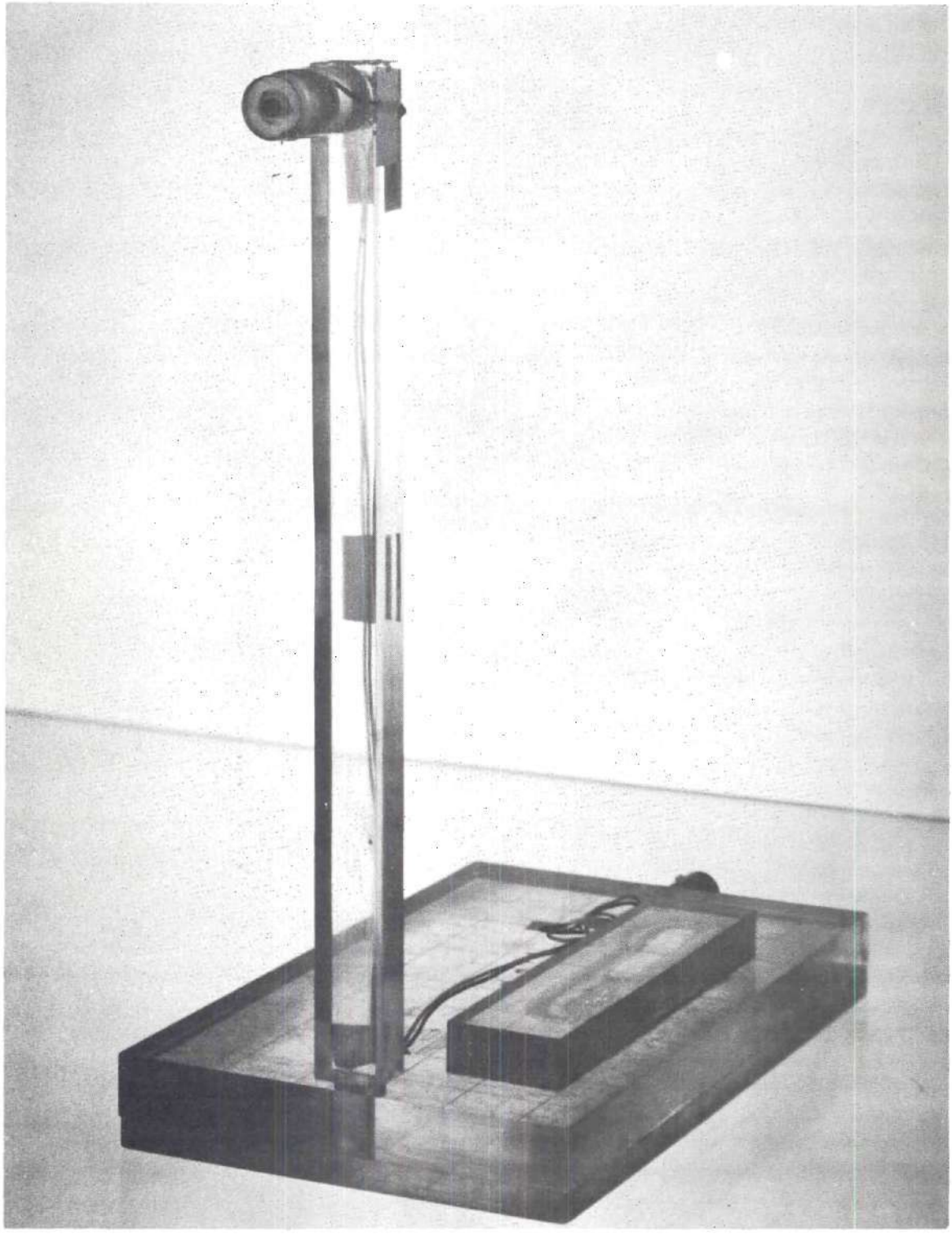

Figure 4. Search Coil.

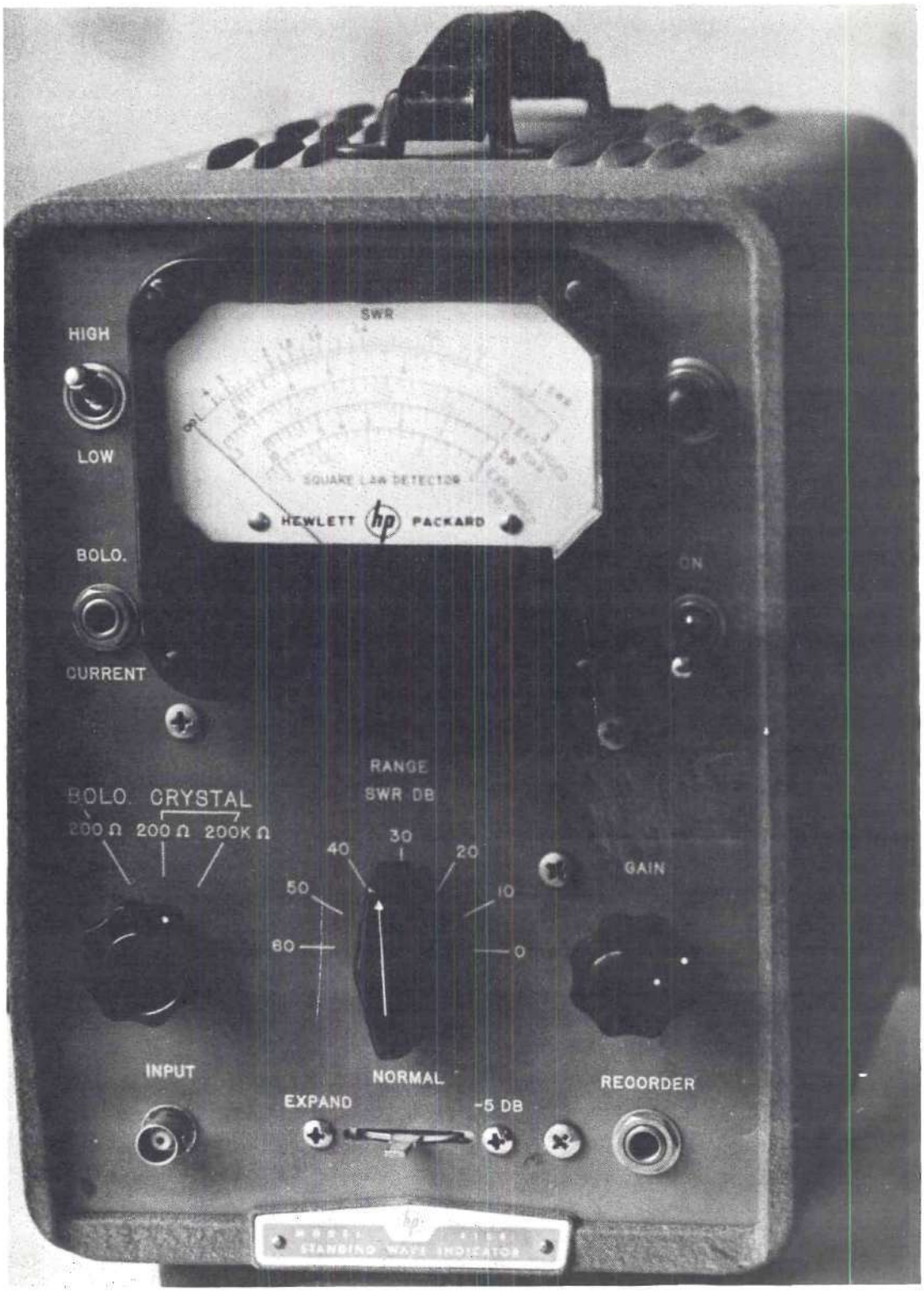

Figure 5. Amplifier and Meter.

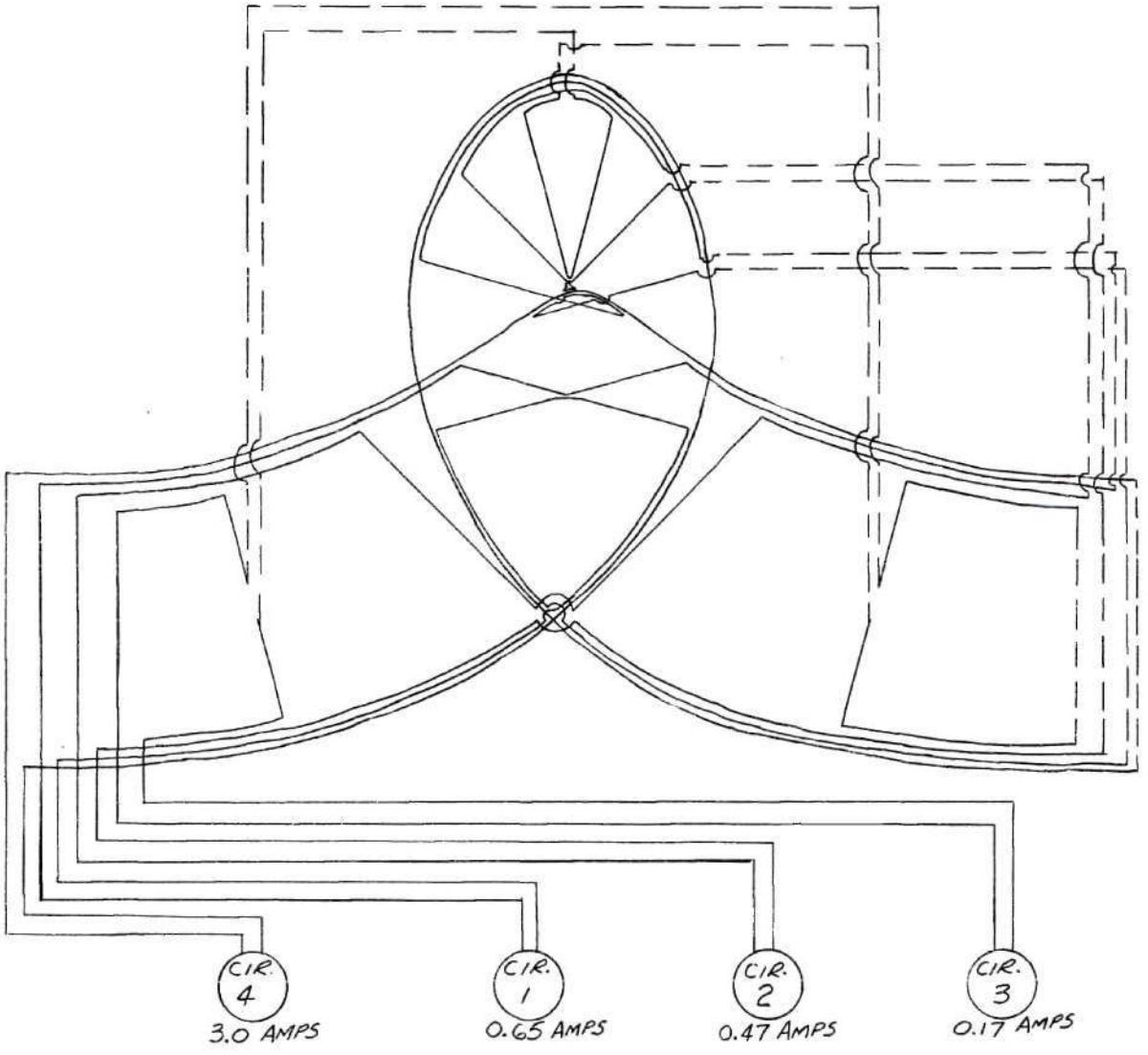

Fig. 6 Wake Model Circuit Diagram

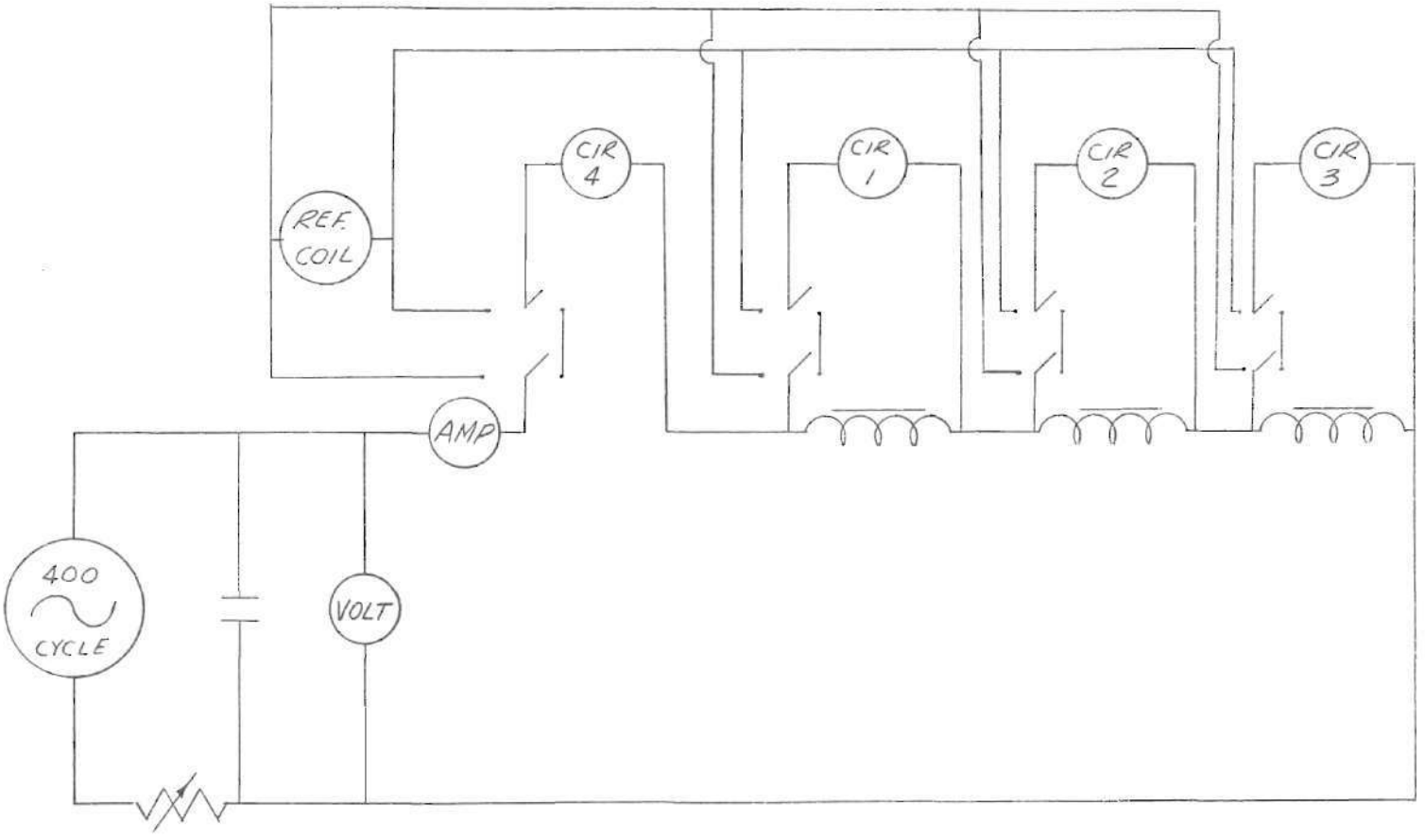

Fig. 7 Electromagnetic Analog Wiring Diagram

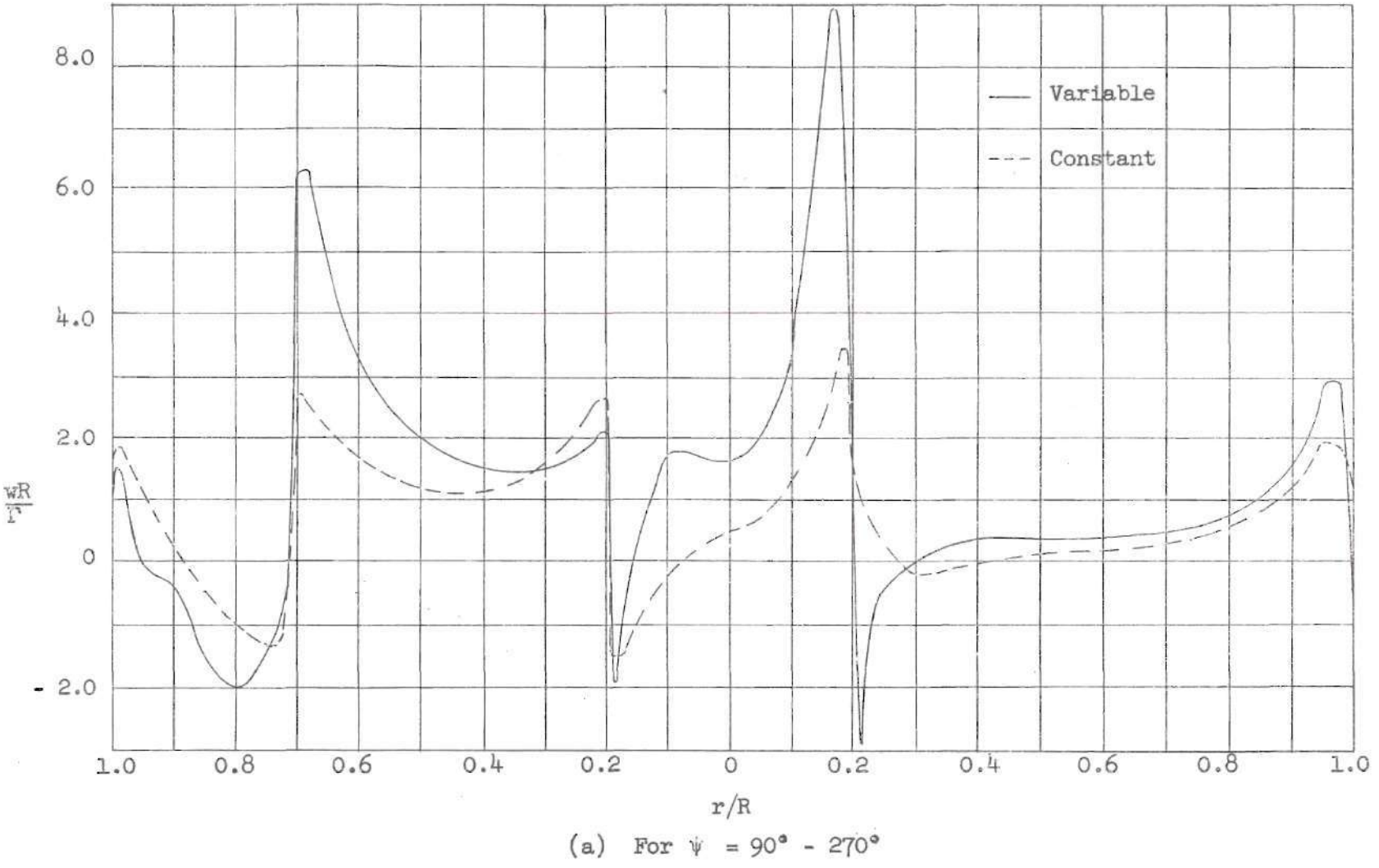

(a) For ψ = 90° - 270°

Fig. 8 Variation of Non-Dimensional Normal Component of Induced Velocity Across Rotor for Constant and Variable Blade Circulation

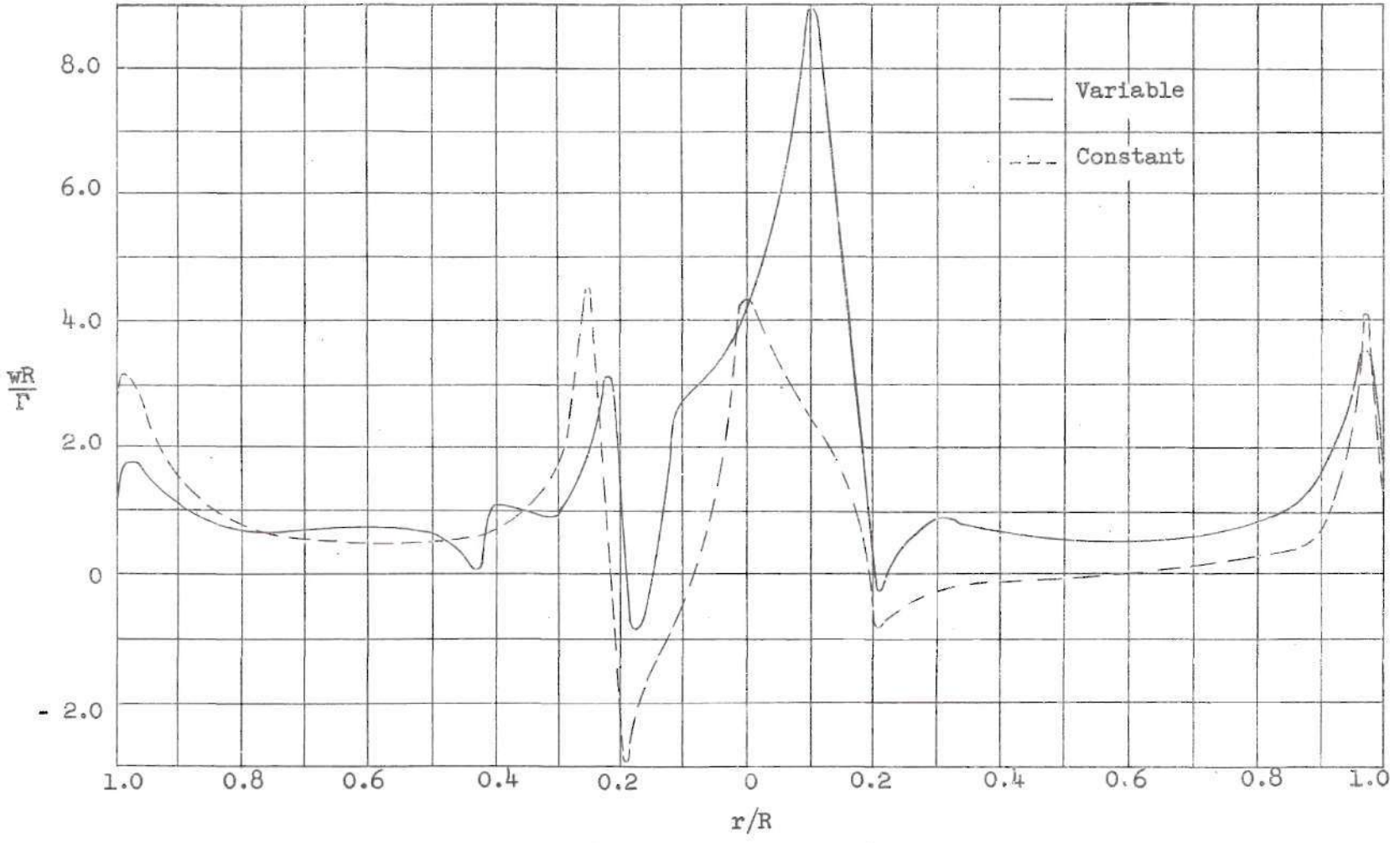

(b) For ψ = 60° - 240°

Fig. 8 (continued)

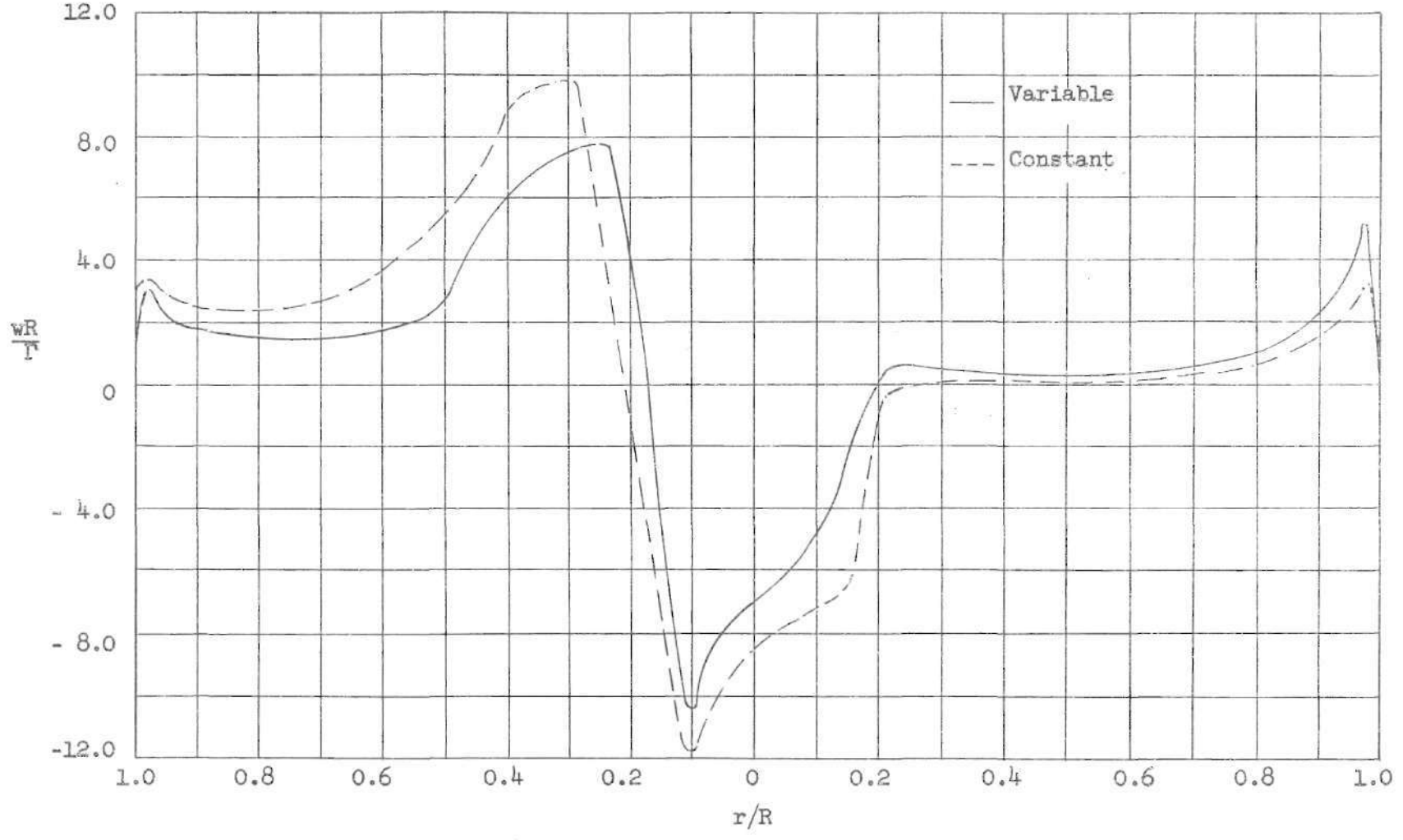

(c) For ψ = 30° - 210°

Fig. 8 (continued)

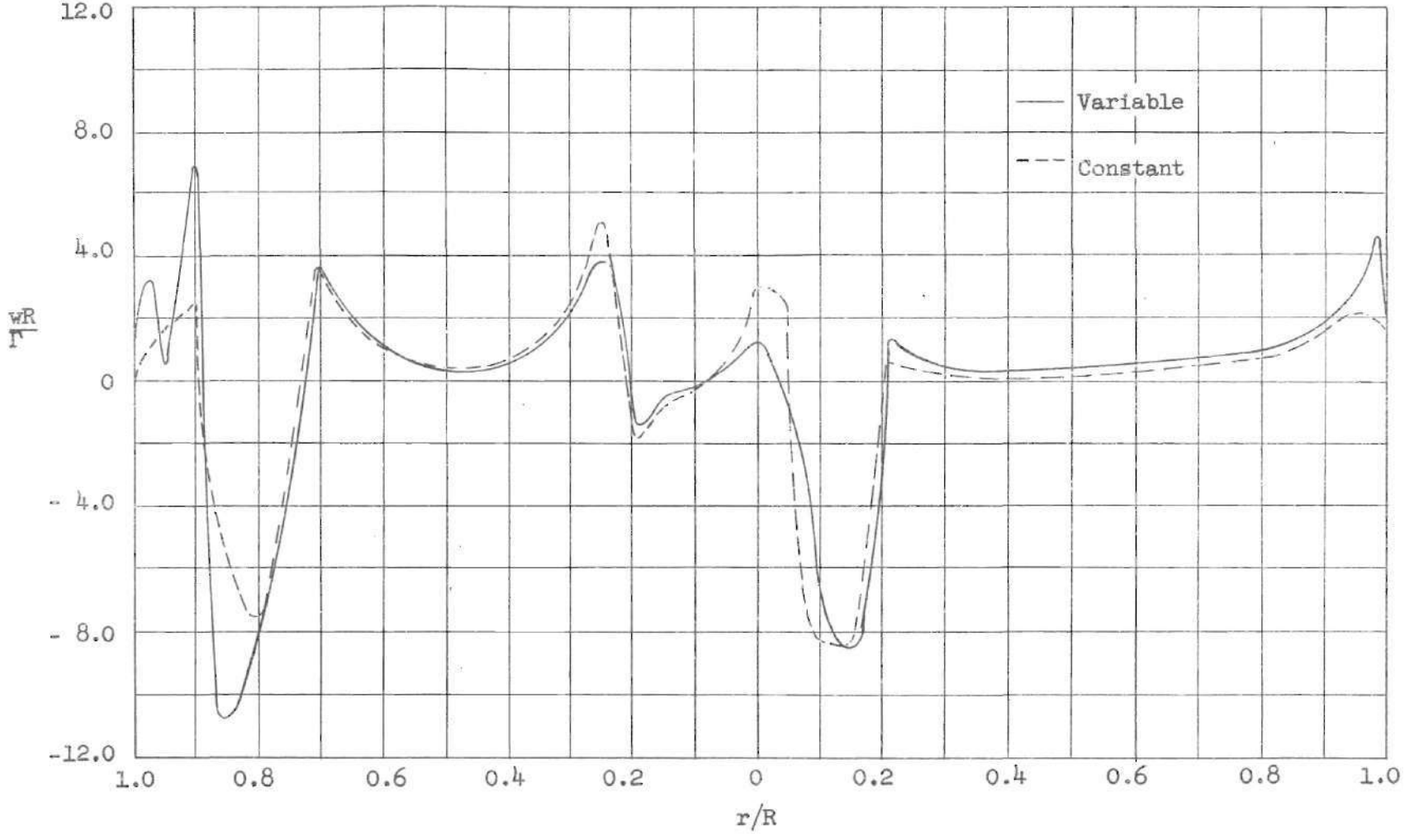

(d) For ψ = 0° - 180°

Fig. 8 (continued)

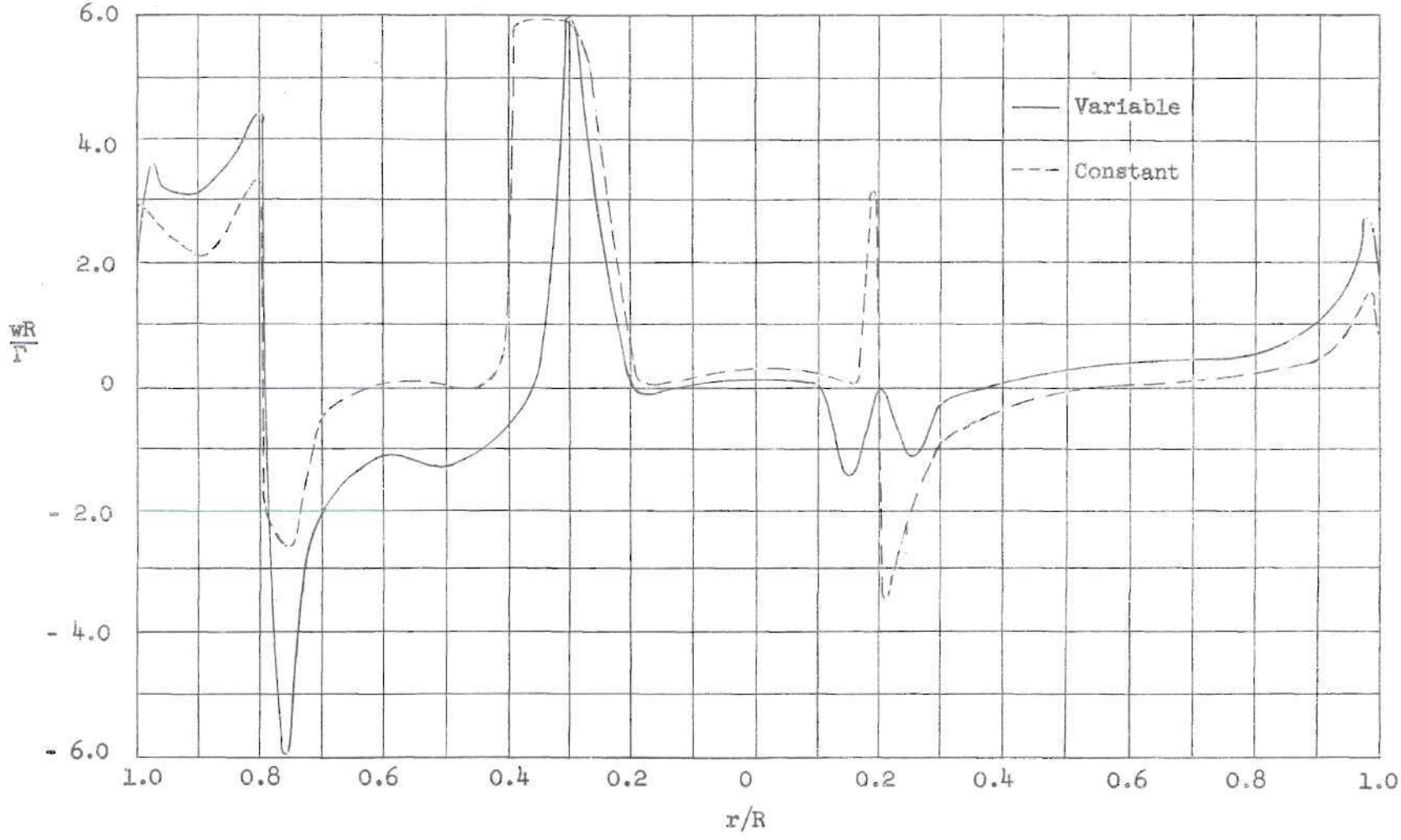

(e) For $\psi = 330° - 150°$

Fig. 8 (continued)

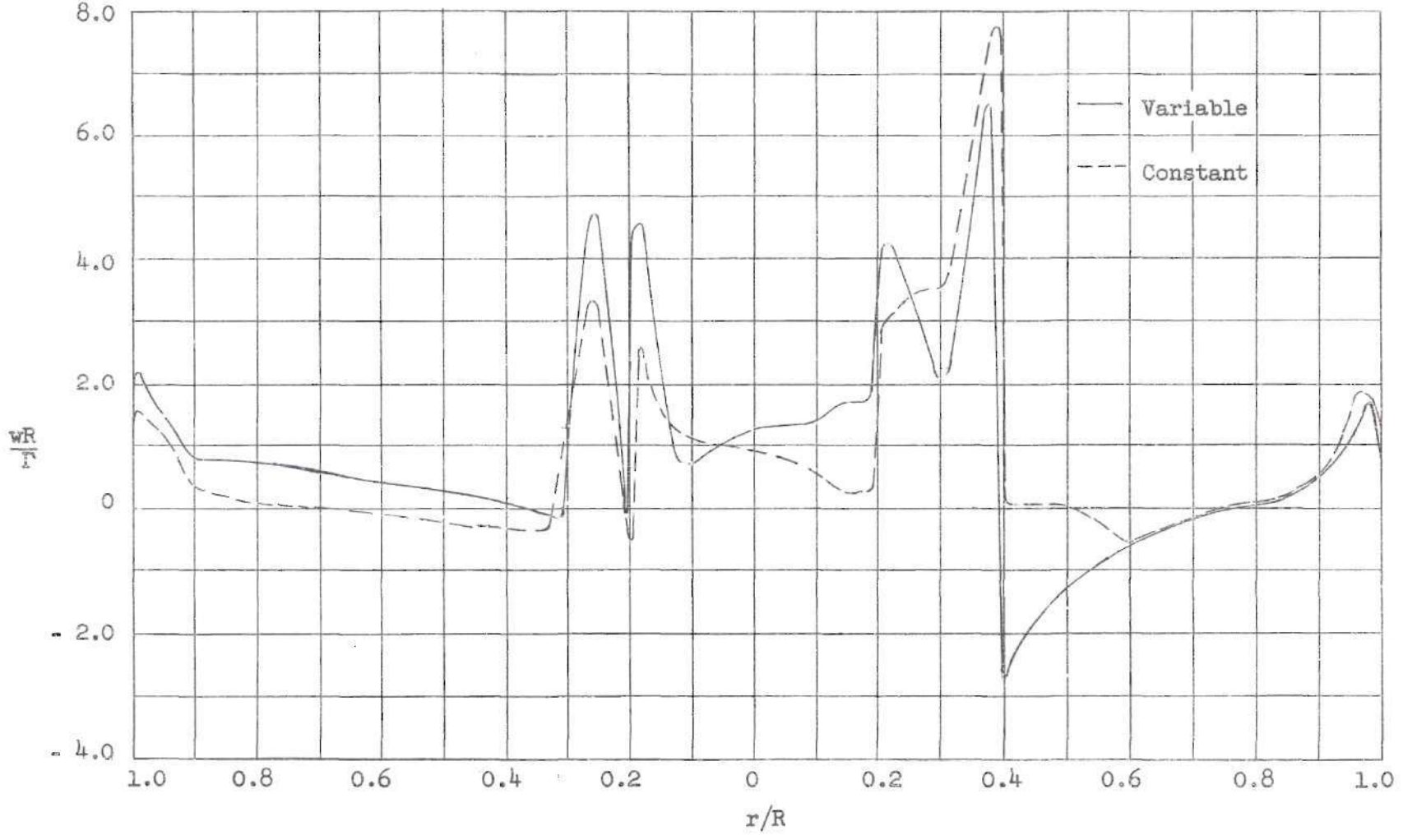

(f) For ψ = 300° - 120°

Fig. 8 (continued)

APPENDIX

CALCULATION OF THE NON-DIMENSIONAL RATIO OF VARIABLE TO CONSTANT CIRCULATION STRENGTH

Assuming constant circulation along the blade radius and lateral harmonic variations with azimuth angle

$$\Gamma = \Gamma_o + \Gamma_1 \sin \psi$$

$$dT = \rho U_T \Gamma \, dr$$

$$T = \frac{b}{2\pi} \int_o^{2\pi} \int_{0.2R}^{R} \rho(\Omega r + \mu \Omega R \sin\psi)(\Gamma_o + \Gamma_1 \sin\psi) \, d\psi \, dr$$

$$T = b\rho \frac{\Omega R^2}{2}(0.96 \Gamma_o + 0.8 \mu \Gamma_1)$$

$$C_T = \frac{T}{\rho\pi R^2(\Omega R^2)}$$

$$C_T = \frac{b}{2} \frac{(0.96 \Gamma_o + 0.8 \mu \Gamma_1)}{\pi \Omega R^2}$$

$$M_T = \int_{0.2R}^{R} \rho(\Omega r + \mu \Omega R \sin\psi)(\Gamma_o + \Gamma_1 \sin\psi) r \, dr$$

$$M_T = \rho \Omega R^3 \left\{ \left[0.3306 \Gamma_o \right] + \left[\frac{0.96 \mu \Gamma_o}{2} + \frac{0.992 \Gamma_1}{3} \right] \sin\psi \right.$$

$$\left. + \left[\frac{0.96 \mu}{3} \Gamma_1 \right] \sin^2 \psi \right.$$

The first harmonic of the thrust moment must be zero.

$$\frac{0.992}{3}\,\Gamma_1 = -\frac{0.96\,\mu\,\Gamma_\circ}{2}$$

$$\Gamma_1 = -1.4516\,\mu\,\Gamma_\circ$$

$$C_T = \frac{b}{2}\,\frac{(0.96\,\Gamma_\circ - 1.1613\,\mu^2\,\Gamma_\circ)}{\pi\,\Omega\,R^2}$$

$$\Gamma_\circ = \frac{2\,C_T\,\Omega\,\pi\,R^2}{b(0.96 - 1.1613\,\mu^2)}$$

$$\Gamma_1 = -1.4516\,\mu\,\frac{2\,C_T\,\Omega\,\pi\,R^2}{b(0.96 - 1.1613\,\mu^2)}$$

$$\Gamma = \frac{2\,C_T\,\Omega\,\pi\,R^2}{b(0.96 - 1.1613\,\mu^2)} - 1.4516\,u\,\frac{2\,C_T\,\Omega\,\pi\,R^2}{b(0.96 - 1.1613\,\mu^2)}\,\sin\,\psi$$

$$\gamma = \frac{\Gamma}{2\,C_T\,\Omega\,\pi\,R^2} = \frac{1}{b(0.96 - 1.1613\,\mu^2)}\left[1 - 1.4516\,\mu\,\sin\,\psi\right]$$

$$\gamma_{\text{constant}} = \frac{1}{b(0.96 - 1.1613\,\mu^2)}$$

$$\gamma_{\text{variable}} = \frac{1.4516\,\mu\,\sin\,\psi}{b(0.96 - 1.1613\,\mu^2)}$$

For $b = 2$ and $\mu = 0.3$

$$\gamma_{\text{constant}} = 0.58445$$

$\gamma_{constant}$ is circuit 4 and was represented with 3.0 amperes of current.

$$\gamma_{variable} = - 0.2545 \sin \psi$$

$$\frac{d \gamma_{variable}}{d \psi} = \text{sheet strength} = - 0.2545 \cos \psi$$

$$\gamma_{15^\circ} = \int_0^{30^\circ} - 0.2545 \cos \psi \; d \psi$$

Integrating this expression every 30 degrees for 360 degrees yields the non-dimensional values of the variable part of blade circulation.

The ratios of variable to constant circulation and the representative currents are given below.

Circuit No.	$\gamma_{var} / \gamma_{const}$	Current(Amperes)
1	0.2176	0.653
2	0.1595	0.468
3	0.0583	0.175
4	1.000	3.000

The desired current was not obtained in all circuits but time did not allow a re-wiring of the current transformers to obtain the exact ratios.

The ratios of $\gamma_{var} / \gamma_{const}$ obtained follow:

Circuit No.	$\gamma_{var} / \gamma_{const}$	Per Cent Error
1	0.1738	20.0
2	0.1349	15.5
3	0.0575	1.2
4	1.000	0.0

BIBLIOGRAPHY

1. Castles, Walter, Jr., and Durham, Howard L., Jr., The Computed Instantaneous Velocities Induced at the Blade Axes by the Skewed Helical Vortices in the Wake of a Lifting Rotor in Forward Flight, Department of the Navy, AD-210 613, March, 1959.

2. Gray, Robin B., Experimental Smoke and Electromagnetic Analog Study of Induced Flow Field about a Model Rotor in Steady Flight within Ground Effect, National Aeronautics and Space Administration, Technical Note No. D-458, August, 1960.

3. Castles, Walter, Jr., Durham, Howard L., Jr., and Kevorkian, Jiriar, Normal Component of Induced Velocity for Entire Field of a Uniformly Loaded Lifting Rotor with Highly Swept Wake as Determined by Electromagnetic Analog, National Advisory Committee for Aeronautics, Technical Note No. 4238.

4. Heyson, Harry H., A Note on the Mean Value of Induced Velocity for a Helicopter Rotor, National Aeronautics and Space Administration, Technical Note No. D-240, May, 1960.